

High-precision magnetic levitation stage for photolithography

Won-jong Kim* and David L. Trumpert†

*SatCon Technology Corporation, Cambridge, MA and †Massachusetts Institute of Technology, Cambridge, MA, USA

In this paper, we present a high-precision magnetic levitation (maglev) stage for photolithography in semiconductor manufacturing. This stage is the world's first maglev stage that provides fine six-degree-of-freedom motion controls and realizes large (50 mm × 50 mm) planar motions with only a single magnetically levitated moving part. The key element of this stage is a linear motor capable of providing forces in both suspension and translation without contact. The advantage of such a stage is that the mechanical design is far simpler than competing conventional approaches and, thus, promises faster dynamic response and higher mechanical reliability. The stage operates with a positioning noise as low as 5 nm rms in x and y , and acceleration capabilities in excess of 1 g (10 m/s²). We demonstrate the utility of this stage for next-generation photolithography or in other high-precision motion control applications. © 1998 Elsevier Science Inc.

Keywords: precision motion control; photolithography; magnetic levitation; mechatronics

Introduction

High-precision position control systems, such as wafer stepper stages for photolithography in semiconductor manufacturing, must provide travel over relatively large displacements in a plane (hundreds of millimeters), small displacements (hundreds of micrometers) normal to the plane, and small rotational displacements (milliradians) around three orthogonal axes. Such a stage must achieve position stability on the order of tens of nanometers. There are significant advantages of a single magnetically levitated moving part for this application, because such a stage can provide all the required motions. A literature review of the class of conventional as well as levitated single-moving-part positioners can be found in Kim.¹

The one moving part also has a simple mechanical structure that yields fast dynamics. These fast dynamics are directly related to high throughput, which is an important design specification for manufacturing equipment.

Several design considerations were raised in the course of discussing specifications and features needed in photolithography. First, a one-moving-part design is more preferable because of manufacturing simplicity and simple dynamics. Second, the motor magnets should be put on the platen to avoid thermal expansion and problematic umbilical cables. Third, a compact design leads to a light moving part; namely, the platen and a small footprint. Fourth, to generate rotational motions, the actuators' lines of force must not pass through the platen's center of mass. Fifth, the lens' field of view above the wafer area must be clear. Thus, we selected a moving magnet-stationary winding stage driven by with four permanent magnet linear suspension motors for prototyping. *Figure 1* is a perspective view of the selected design concept. This design has the following advantages:

Address reprint requests to Dr. W.-J. Kim, SatCon Technology Corp., 161 1st St., Cambridge, MA 02142, USA. E-mail: kimwj@worldnet.att.net

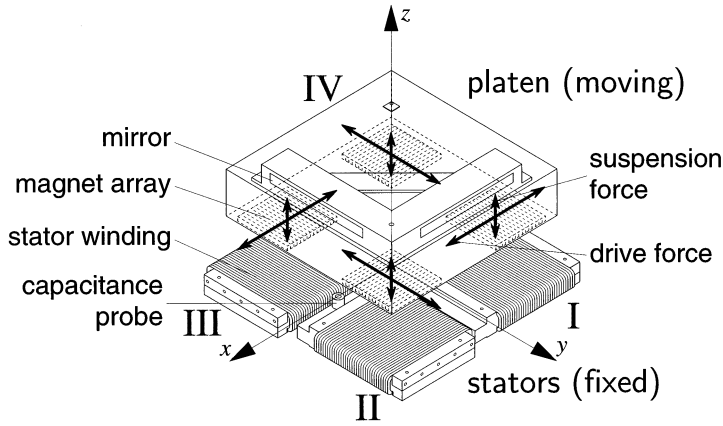


Figure 1 Perspective view of the magnetically levitated stage; the motor forces acting on each magnet array are shown as arrows; the stators are labeled I through IV

- no umbilical cables to the platen except for the ground wire for the capacitive gap sensors;
- symmetry in the x - and y -directions;
- no overhung steel targets for electromagnets or preload magnets; i.e., nothing above the platen;
- no heat dissipation on the platen (except for negligible eddy current loss in the magnets) to minimize deformation caused by thermal expansion; and
- heat generated by the stators easily removed to the mounting table by conduction.

We have designed a novel permanent magnet linear motor to provide drive force as well as suspension force for a magnetically levitated wafer-stepper stage.^{1,2} The linear motors consist of Halbach-type³ magnet arrays attached to the underside of the levitated puck and coil sets attached to the fixed machine platform. The platen is levitated without contact by four such permanent-magnet linear motors, which provide both suspension and drive forces. By coordinating the forces applied by each motor, the stage can be accurately controlled in six degrees of freedom. The platen mass of 5.58 kg is supported against gravity by the combined forces of the four motors. The present design has a travel of 50 mm in x and y , a travel of 400 μm in z , and is capable of milliradian-scale rotations about each of these three axes. Detailed fabrication issues of the stage can be found in Kim¹ and Kim et al.⁴ and are not repeated here. The electromechanics and configuration based on our theory and design has also been adopted in a scanning stage built by Mike Holmes at the University of North Carolina—Charlotte.⁵

This paper presents the working principles underlying the stage operation, and experimental data demonstrating the stage performance capabilities. In the following section, an overview of the mag-

netic levitation stage is given. The next section describes the real-time control of the stage. Test results are presented and discussed in the last section.

High-precision planar magnetic levitator

Figure 2 is a photograph of a prototype magnetic levitation stage designed and implemented by the authors. The stage position in the plane is measured with three laser interferometers with sub-nanometer resolution. The stage position out of the plane is measured by three capacitance gauges with nanometer resolution. At present, the stage is operational with a positioning noise of 5 nm rms in x and y , and is demonstrating acceleration capabilities in excess of 1 g (10 m/s^2).

Working principles

Figure 3 depicts the dynamic equilibrium around which the levitator operates and is stabilized. The peaks of idealized sinusoidal stator currents are shown as \times into the page and \cdot out of the page. We also show the associated north (N) and south (S) poles generated by these currents. At a fixed time, if we generate the current approximately by a sinusoidal distribution in the y -direction, as illustrated in Figure 3, there is a vertical repulsive force between the same magnetic poles of the magnet array and the current distribution (i.e., corresponding north to north and south to south). This vertical repulsive force lifts the platen against gravity. The vertical motions of the platen are stable because of a positive magnetic spring effect between the magnet array and stator currents. The incremental equation of motion in the vertical direction is derived in Kim¹ as follows:

$$5.58 \frac{d^2 \tilde{z}}{dt^2} + 13600 \tilde{z} = \tilde{f}_z \quad (1)$$

where \tilde{z} and \tilde{f}_z are incremental vertical position and force, respectively. However, because this equilibrium is unstable in the lateral direction (in

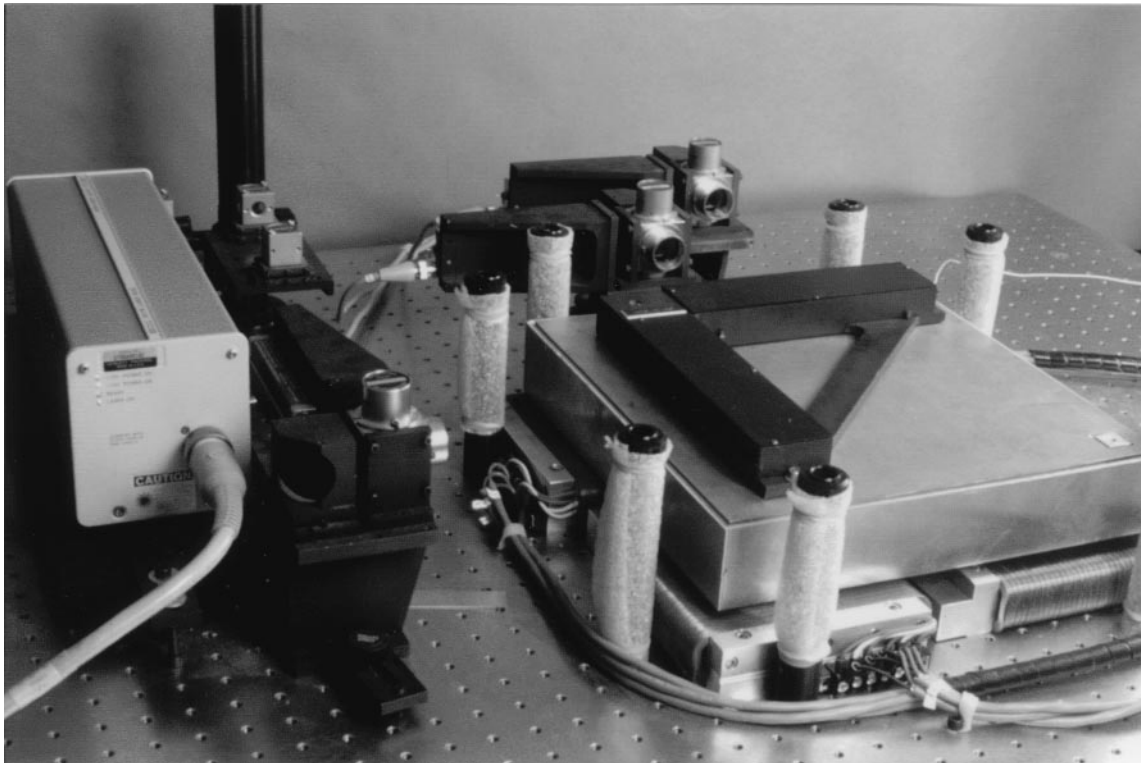


Figure 2 Photograph of high-precision magnetic levitation stage for photolithography; the stage is driven by the four stators attached to the optical table; the laser source and optics can be seen to the left and behind the stage; the three laser paths reflect off the stick mirrors housed in the black assembly on top of the stage; the vertical posts act as mechanical stops

the y -direction in the figure), we need active feedback control to stabilize the motion of the platen around this dynamic equilibrium. Conceptually, we can control the magnitude of the vertical force by changing the magnitude of the stator currents, and control the lateral force by commutation. See Kim,¹ and Trumper et al.² for more details. This

two-force linear levitation motor can be considered as a technical building block that can be applied to a wide range of new positioning systems.

The four motors in *Figure 1* collaboratively generate all six-degree-of-freedom motions for focusing and alignment and large two-dimen-

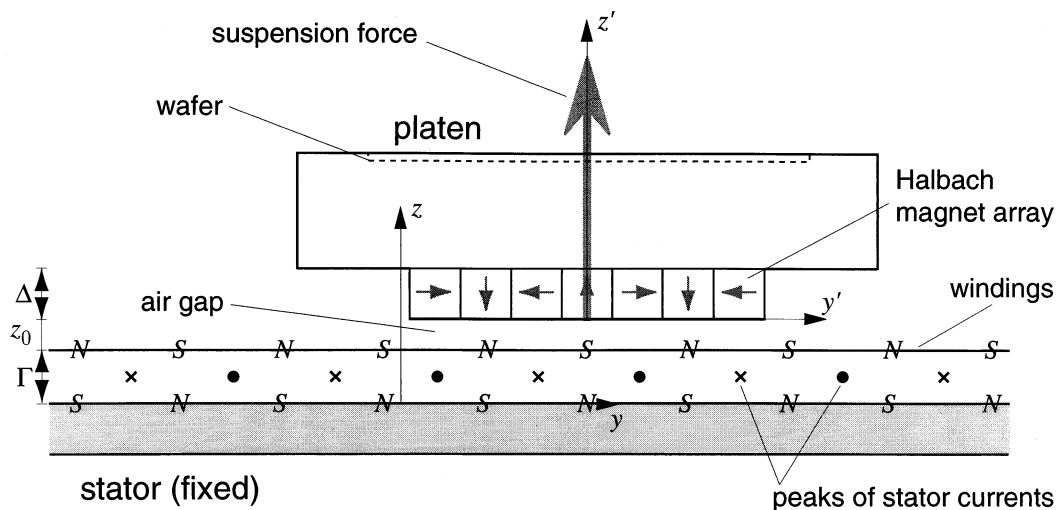


Figure 3 Suspension of the platen in dynamic equilibrium; the peaks of the stator currents are indicated as dots and crosses; the corresponding north and south poles are shown

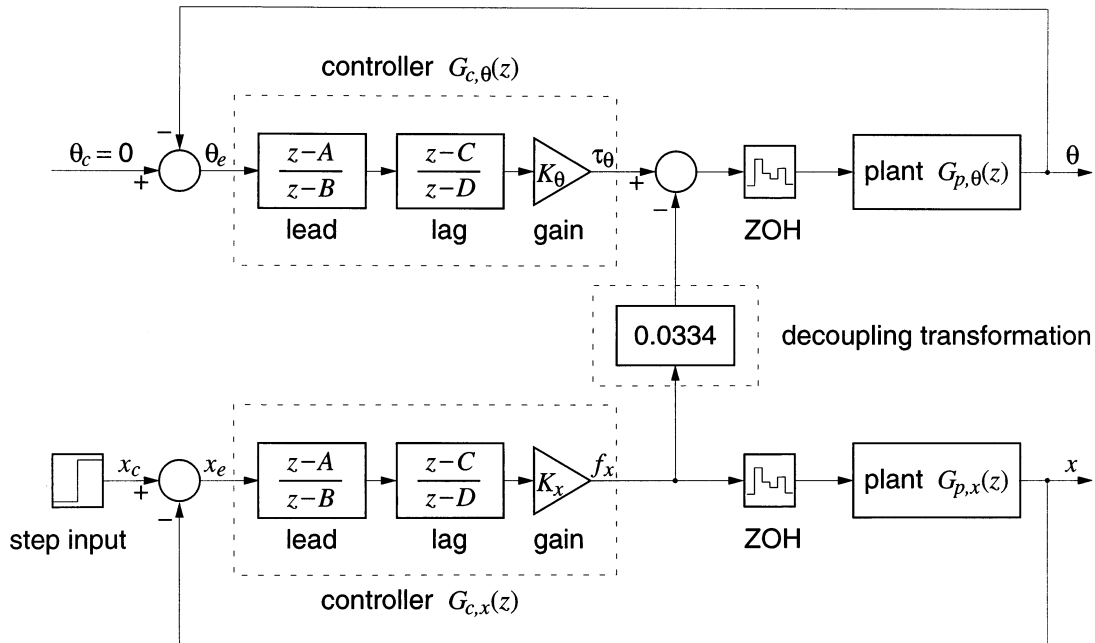


Figure 4 Discrete-time lead-lag compensators with decoupling transformation

sional (2-D) step and scanning motions for such high-precision positioners as a wafer stepper stage in semiconductor manufacturing. Two of the motors (I and III) drive the stage in the x -direction, and the other two (II and IV), in the y -direction. The motor forces are coordinated appropriately to control the remaining degrees of freedom.

Parameters and specifications

For our three-phase permanent magnet linear motors, the parameters have the following values: magnet remanence, $\mu_0 M_0 = 1.29$ T, pitch $l = 25.6$ mm, and the nominal motor air gap $z_0 = 250$ μm . The magnet array thickness is $\Delta = l/4$, and the winding thickness is $\Gamma = l/5$.

To drive the motors, we implement linear transconductance power amplifiers, with maximum current and voltage ratings of ± 1.5 A at ± 22 V.¹ The nominal power dissipation per motor required to carry the stage weight is 5.4 W at the 0.5-A nominal peak phase current. The total suspension power coefficient of the stage is, thus, 7.2 mW/N². The resistance and the self-inductance of one phase winding are 14.4 Ω and 3.44 mH, respectively.

Instrumentation

Control algorithms are implemented digitally in a Pentek 4284 board based on the Texas Instrument TMS320C40 digital signal processor. A RadiSys 80486-100 MHz VME PC takes care of the user interface, such as monitoring levitator state vari-

ables and command interpretation. The PC and the digital signal processor communicate with each other over the VMEbus using dual-port shared RAM residing on the Pentek 4284 board. On the VMEbus exist three channels of Hewlett-Packard 10897A laser axis boards for horizontal motions and a DATEL DVME-622 12-bit digital-to-analog (D/A) converter board. There is a MIXbus local to the digital signal processor connected to a Pentek 4245 16-bit analog-to-digital (A/D) converter board.

We have three ADE 3800 systems including three ADE 2810 capacitance probes for vertical motions. The output ranges of the ADE 3800 systems are modified to be ± 7.5 V to match the input voltage swing of Pentek 4245 A/D converter board. This maximizes the position sensitivity. The zero point of the gauging system is set at the 450- μm air gap between the top surfaces of ADE 2810 capacitance probes and the targets on the bottom side of the platen. The scale factor (displacement-to-voltage ratio) is determined by the sensing range that is 200 μm –700 μm . The air gaps between the capacitance probes and their targets are nominally 500 μm . The air gaps between the stator windings and the magnet arrays are nominally 250 μm . Because the nominal sensor air gap subtracted by the motor air gap (250 μm) is larger than the minimum of the capacitance probe sensing range (200 μm), the system metrology functions properly, even when the magnets on the platen are in contact with the stators, which is the case at start-up. Thus, the

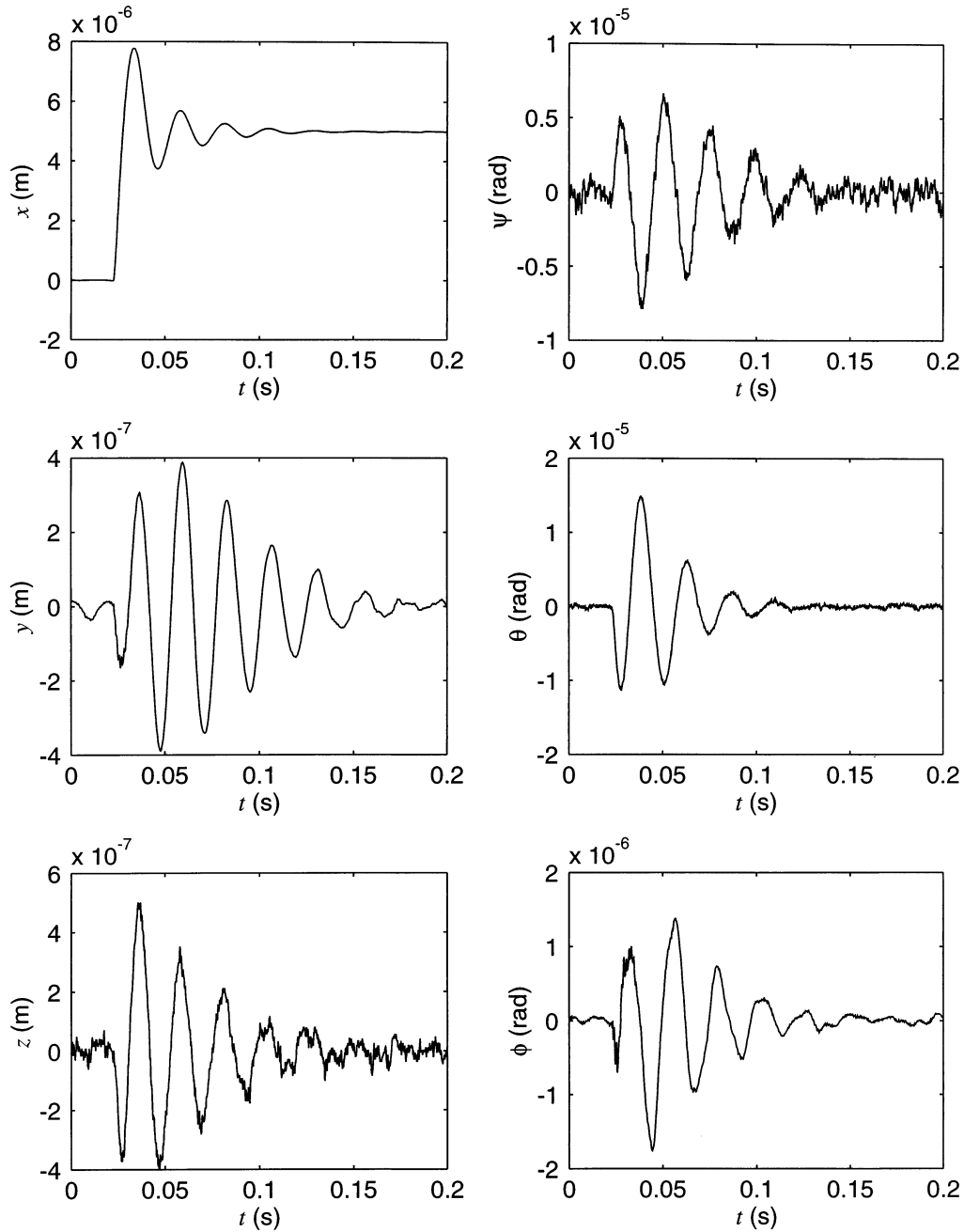


Figure 5 5- μm step response in x without decoupling transformation

stage can properly levitate from a power-off condition, because the probe signals are “live” over the whole allowed travel range. In the following section, we describe the real-time control of the magnetic levitator.

Real-time digital control

Initial testing procedure

Because vertical modes are stable at the operation point we set, it is a proper approach to attempt to close the vertical control loop first.

We mechanically confine the unstable lateral motions for the initial vertical motion testing. This confinement is achieved with Mylar tapes to fix four corners of the top surface of the platen with respect to the eight bumper posts (visible in *Figure 2*). Because the nominal lateral forces at the operation point (a dynamic equilibrium) are zero, the tapes have only to withstand small perturbation forces and lateral forces caused by misplacement of the platen from the equilibrium point resulting from the tape compliance. The three-degree-of-freedom vertical modes are es-

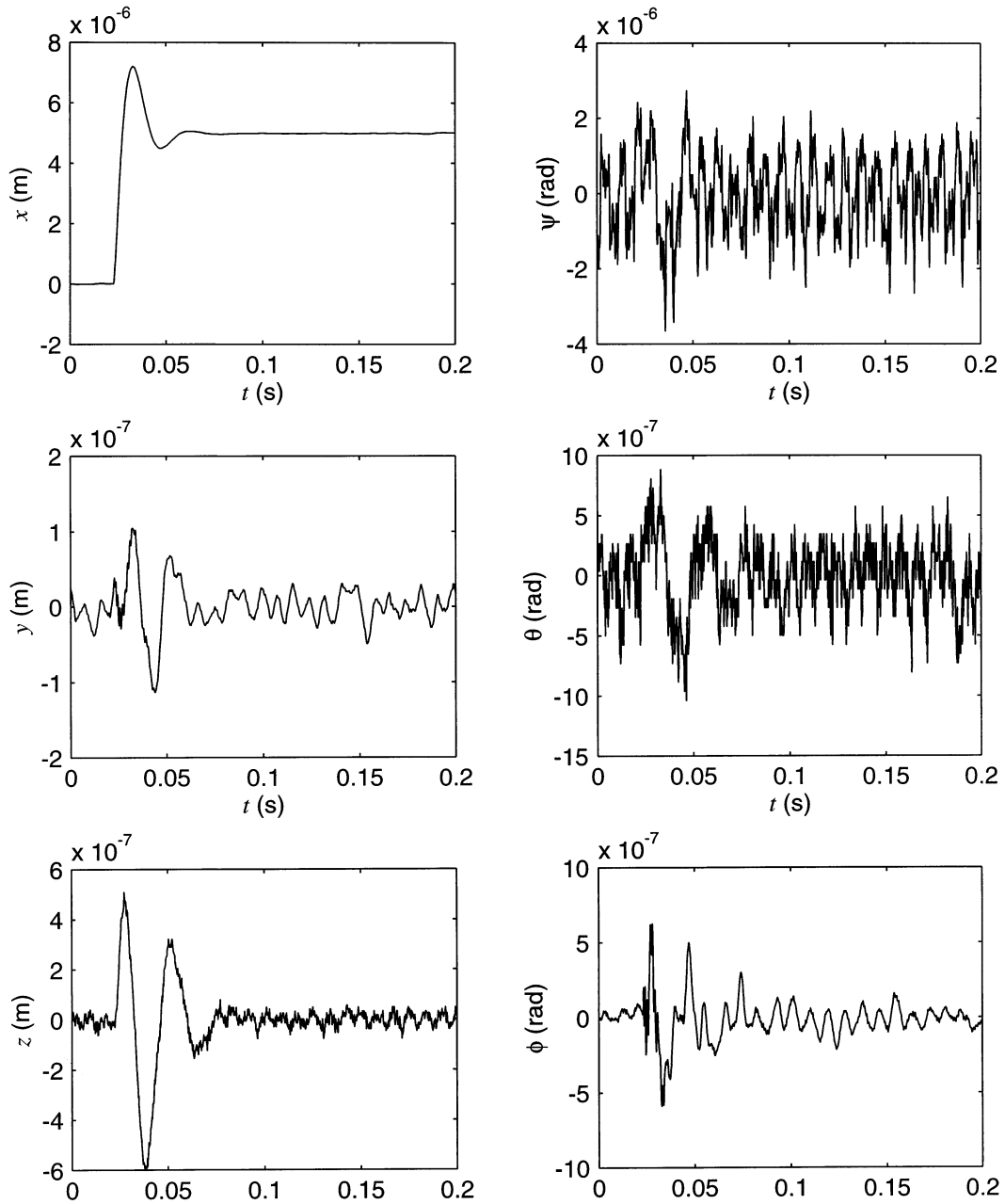


Figure 6 5- μm step response in x with decoupling transformation

essentially free from constraint with this scheme. The dynamics attributable to Mylar tapes are very slow and, thus, negligible. After closing the loop for the vertical translational motion, the other two control loops for rotational motions ψ and θ about the x - and y -axes respectively, are closed. Finally, we close the other three degrees of freedom, x , y , and ϕ . In this paper, we follow the xyz convention, which is commonly used in engineering applications, to define Euler angles.⁶ For small angular motions in our levitator, the Euler angles ψ , θ , and ϕ can be considered as rotational angles around x , y , and z -axes, respectively.

Decoupled control

Figure 4 is a block diagram of the decoupled discrete-time lead-lag controllers for x and θ with $A = 0.96300$, $B = 0.68592$, $C = 0.99624$, and $D = 1$. The gains K for the six axes x , y , z , ψ , θ , and ϕ are 2.2261×10^6 N/m, 2.2261×10^6 N/m, 2.3141×10^6 N/m, 2.2504×10^4 N/rad, 2.2504×10^4 N/rad, and 3.9804×10^4 N/rad, respectively. Because of the geometric symmetry in x and y of the levitation system, they have identical gains. The same is true for the controllers for ψ and θ . The sampling rate is 5 kHz.

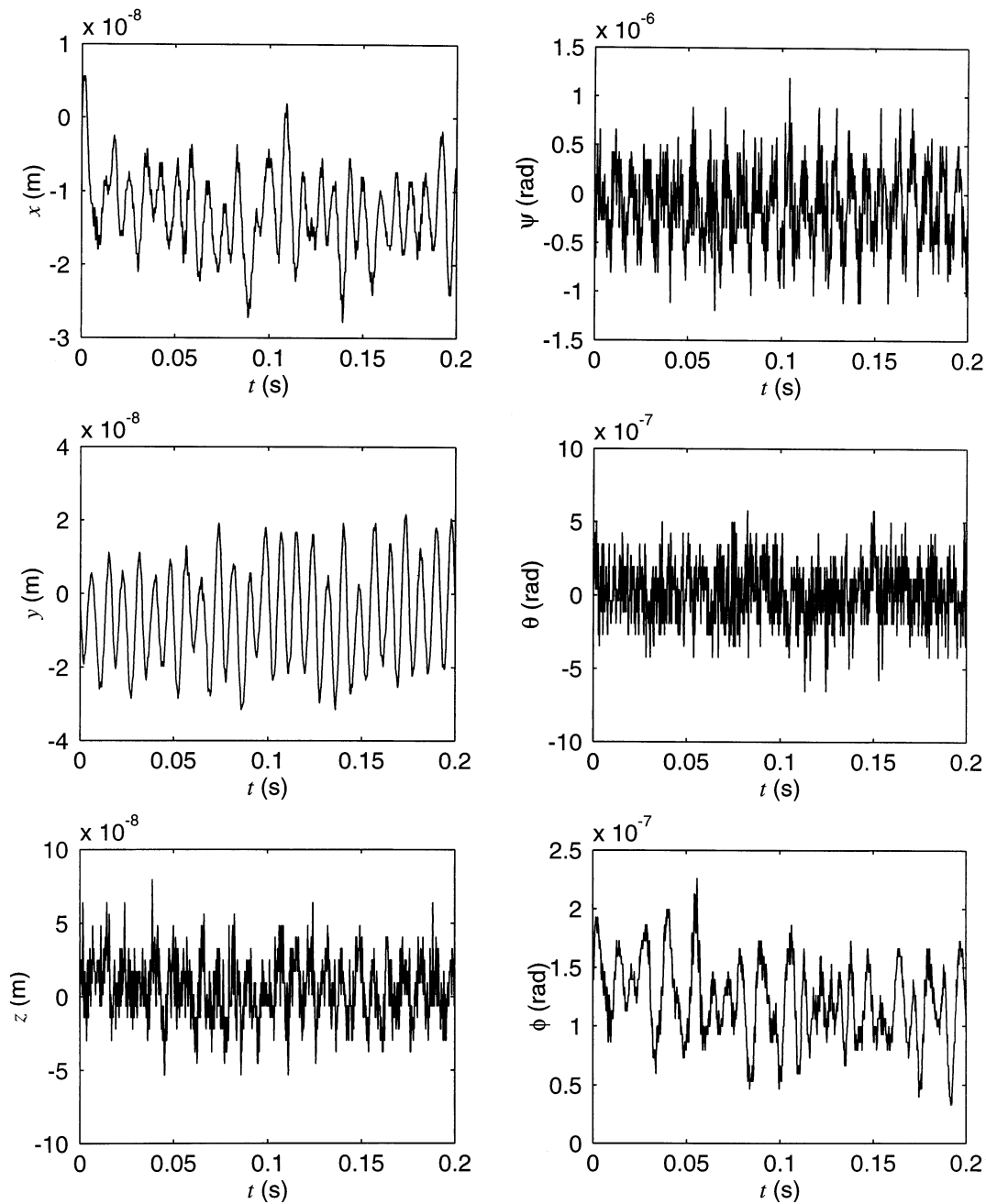


Figure 7 Positioning noise in all six axes

Figure 5 shows a 5- μm step response in x with these lead-lag compensators without the decoupling transformation denoted in Figure 4. All the six-axis controllers are operational in this experiment. Note that the platen dynamics are coupled in six degrees of freedom. Because of this coupling nature of the platen, there are perturbed motions in all the other five axes. The step response also shows that the system has only about 20° phase margin as compared with a design value of 45° , and this response shows correspondingly more ringing compared with the computer simulation.

This phenomenon of the loss of phase margin originates from an unmodeled coupling effect. Specifically, the center of mass of the platen is not on the plane that encloses the actuation points of forces of the linear motors. Thus, any linear motion in the x -direction, for example, generates perturbed rotational motion around the y -axis. It is the reason Figure 5 shows large angular position fluctuations in θ , the rotation around the y -axis. We calculated the vertical offset of the platen center of the mass. It is above the actuation plane by 33.4 mm. It is not easy to model these couplings exactly, but we can at least correct this deterministic perturbation by subtract-

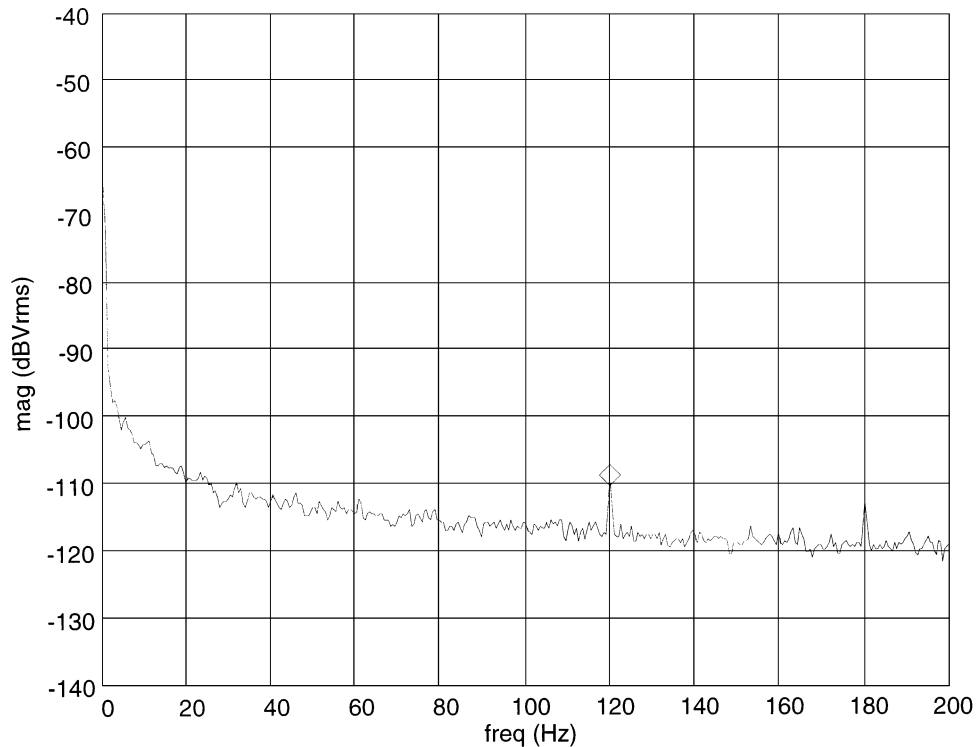


Figure 8 Power spectrum of the floor vibration effect as transmitted through the optical table

ing the erroneous torque around the y -axis that is the linear force in the x -direction multiplied by the 33.4-mm moment arm, as indicated in *Figure 4*. The perturbed torque around the x -axis is corrected likewise. *Figure 6* shows another 5- μm step response with this decoupling transformation implemented with the same lead-lag compensators above. We can see that the perturbed motions in other axes and the ringing are significantly decreased. It shows now a typical step response of a second-order system with damping ratio, $\zeta = 0.5$ as designed.

Test results

We provide test results of positioning noise, small repetitive steps, and fast large steps of the magnetic levitation stage in this section.

Positioning noise

Figure 7 shows the position regulation result using the decoupled lead-lag controllers designed above. The platen's position is held at the origin in the global coordinate frame. The positioning noises in x - and y -axes are on the order of 5 nm rms. The positioning noise in ϕ is 0.05 μrad rms. The vertical displacement z shows a 70-nm position error envelope, which is about 10-nm-order rms positioning noise. The A/D converter electronics noise is primarily responsible for the increased positioning noise in z , relative to x and y , which are measured with subnanometer resolu-

tion by means of our laser interferometer system. The A/D quantization levels of 7.6 nm per least count are visible in the z data. This is far coarser than the interferometer channels' least count of 0.6 nm.

The test result in *Figure 7* also has a dominant 120-Hz noise. Lab floor vibration caused by a large transformer in the lab, or heating, ventilation, and air-conditioning (HVAC) equipment located in the next room is believed to generate this noise. *Figure 8* shows a power spectrum of the floor vibration effect as measured with an accelerometer on the top surface of the optical table visible in *Figure 2*. The floor vibration of our lab also includes other lower frequency components at 7.5, 8, 15, and 28 Hz. A more detailed trace of this floor vibration can be found in Ludwick.⁷ This vibration is attenuated by an air spring isolation system, but is still dominant in the error motions.

50-nm repetitive steps

Figure 9 shows 50-nm repetitive steps in x . This test result clearly shows that the resolution of the stage is better than 10 nm. Thus, the resolution versus the travel range is better than one part in 5 million in the x - y plane. The stage shows no hysteretic error, because it is free from sliding friction.

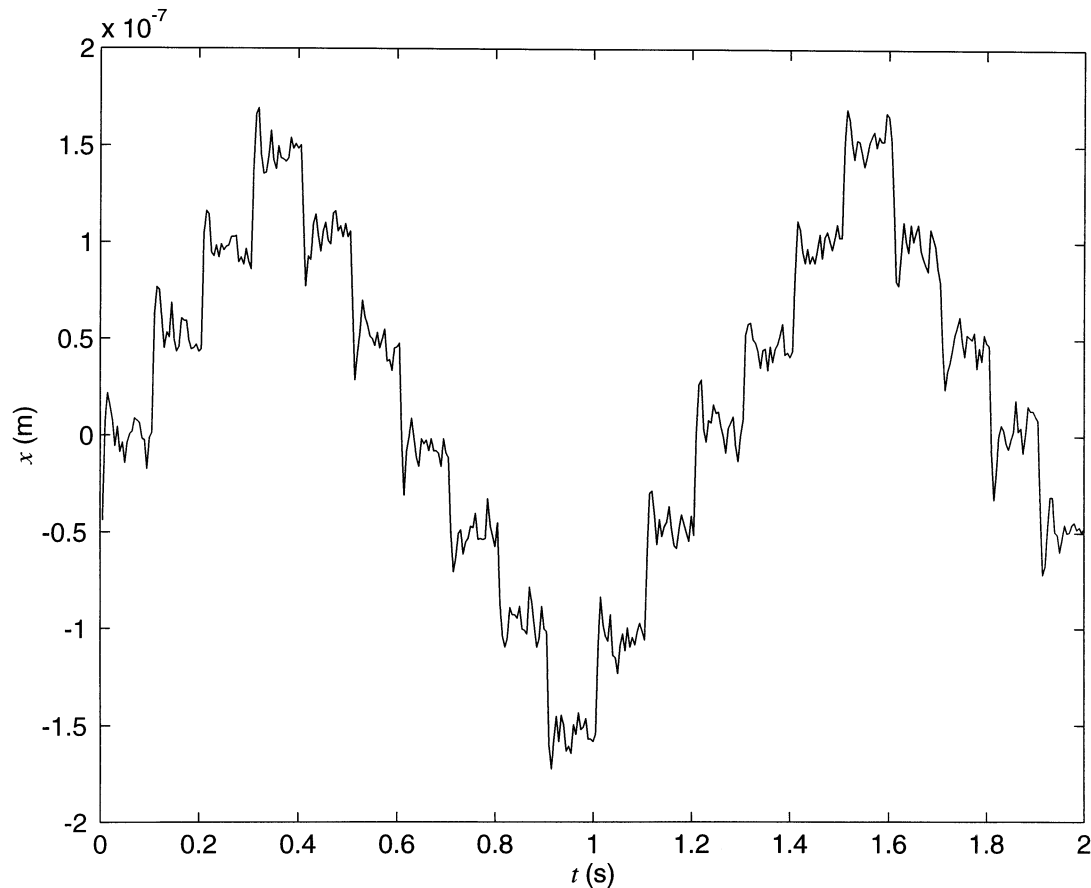


Figure 9 50-nm repetitive steps of stage in x -direction

20-mm steps

To demonstrate our stage's motion capability, we present double 20-mm steps in y in *Figure 10*. We accelerate the platen at $1\ g$ ($10\ \text{m/s}^2$) until its velocity reaches the maximum slew rate of $200\ \text{mm/s}$ of the laser head we use. The platen moves at this constant velocity for $80\ \text{ms}$ and is decelerated at $1\ g$. This motion trajectory is typically referred to as a trapezoidal velocity profile. So, a 20-mm step command completes in $120\ \text{ms}$.

Figure 10 also shows the dynamic coupling effect to the other five degrees of freedom during the 20-mm steps in y . In the future, better modeling of the coupled dynamics with accurate estimations of the platen center of mass and rotational inertias will be required to minimize erroneous forces and torques in other axes. Two error motion profiles in each axis beginning at about $t = 0\ \text{s}$ and $t = 0.4\ \text{s}$ are almost identical, as should be the case given the identical reference changes at these two times. The small difference between the two most likely originates from the nonuniformity of the stator fabrication, because the platen has moved $20\ \text{mm}$ between the first and second stages.

Figure 11 shows details of the same data presented in *Figure 10* from $t = 0.6\ \text{s}$ to $t = 1\ \text{s}$. We again observe the dominant 120-Hz noise component described earlier in this section. The present lead-lag controllers need roughly $250\ \text{ms}$ more to bring the errors in all six axes within their steady-state positioning noise level. This settling time can be reduced by control design. First, move the dominant closed-loop pole more deeply into the left half s -plane by sacrificing phase margin by moving the lag zero to the left in the s -plane. Second, increase the whole closed-loop system bandwidth, which is limited by system structural resonances. Fine-tuning of the controllers to optimize dynamic performance is another area for follow-on work.

Demonstrations

We have also demonstrated that the stage can generate motions typical of a wafer stepper. The platen makes step-and-settle motions described above in the positive y -direction, steps over in the positive x -direction, makes step-and-settle motions in the negative y -direction, and so on. The platen can also follow a circle with 30-mm diam-

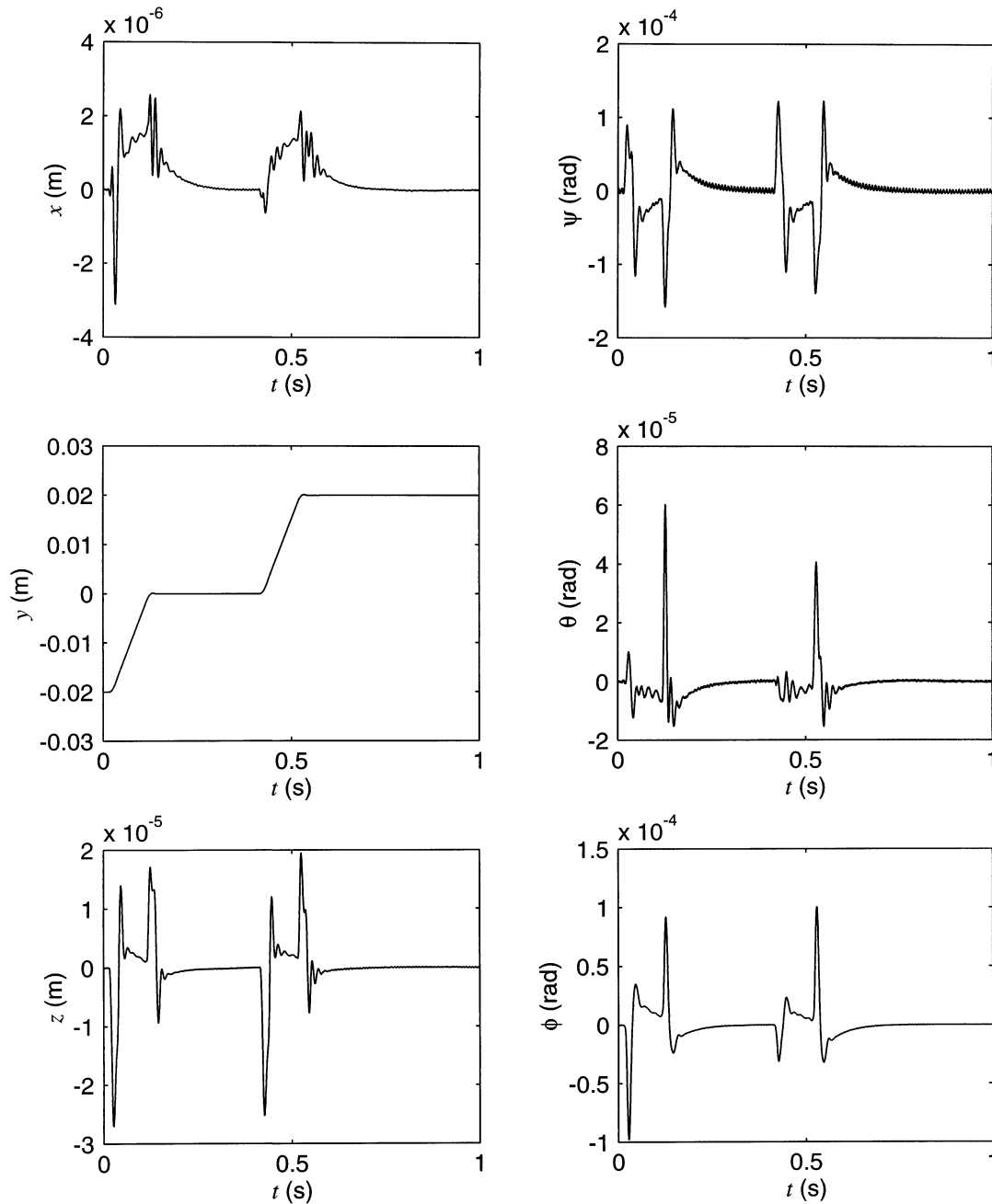


Figure 10 20-mm steps in y on a trapezoidal velocity profile

eter in 1 second. The purpose of this demonstration is to show this magnetic levitation system can generate user-specified 6-axis motions with pre-determined paths having large travel in the plane.

Conclusions

We have designed and implemented the world's first *flying puck*, high-precision, six-degree-of-freedom, magnetic levitator with large 2-D motion capability for photolithography in semiconductor manufacturing. The magnetically levitated platen

generates all the required small motions for focusing and alignments, as well as large planar motions for wafer positioning. This magnetic levitation stage can be readily used in a clean room or a vacuum chamber, because there is no wear particle generation, and no lubrication is required. This design is also highly suitable for vacuum environments, because the heat generated in the motors is in the fixed frame and, thus, can be readily removed by material conduction.

Furthermore, there is no backlash, because the levitation system uses no intermediate power

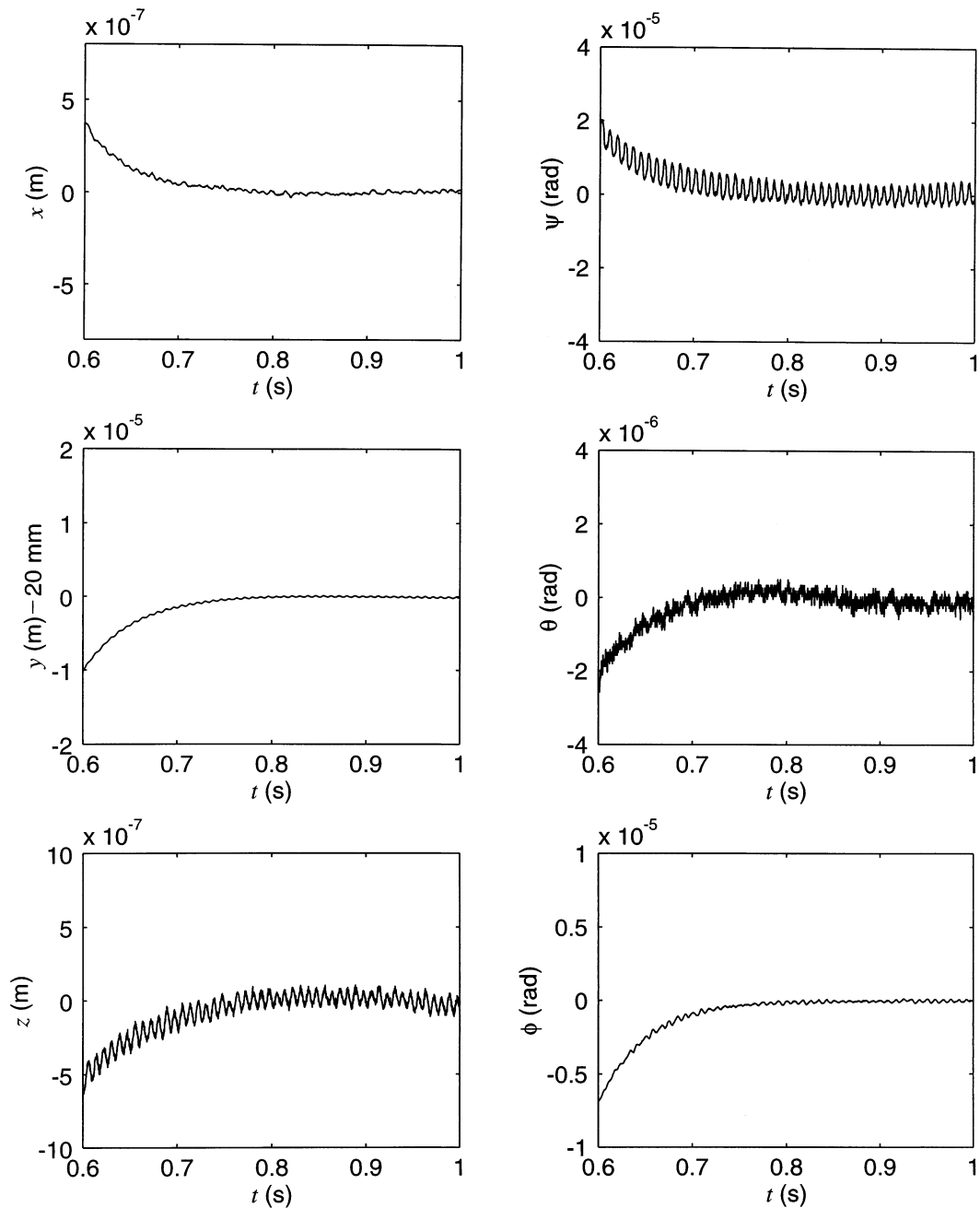


Figure 11 Details of the 20-mm steps in y from 0.6 to 1 second to show the fine-settling behavior

transmission devices such as lead screws. Thanks to the lack of friction or stiction, the position accuracy depends primarily upon the fundamental limits of metrology and control. Another advantage is that no fine finishing of surfaces of mechanical parts, such as for precision bearings, is necessary. This simplifies the production process and reduces the manufacturing cost.

The magnetic levitation stage has been tested successfully. We implemented decoupled lead-lag digital controllers in a TMS320C40 digital signal processor. The sampling rate of the system is 5 kHz. The control loop for the levitator has been

closed at a 50-Hz bandwidth. Important experimental achievements include 5-nm rms positioning noise in x and y , 10-nm rms positioning noise in z , 20-mm steps following 120-ms references, and 1- g acceleration. We, thus, have demonstrated that this magnetic levitator is a promising candidate as the high-precision positioning stage in next-generation semiconductor manufacturing.

Acknowledgments

Portions of this work are part of a thesis submitted by W.-J. Kim¹ for the Ph.D. in electrical engineer-

ing and computer science at the Massachusetts Institute of Technology, Cambridge, Massachusetts. This work is supported in part by a contract from Sandia National Laboratories under subcontract no. AH-4243 and in part by a scholarship from Korean Ministry of Education to W.-J. Kim and a National Science Foundation Presidential Young Investigator Award (DDM-9496102) to D. L. Trumper.

References

- 1 Kim, W.-J. "High-precision planar magnetic levitation." Ph.D. thesis, Massachusetts Institute of Technology, Cambridge, MA, June 1997
- 2 Trumper, D. L., Kim, W.-J. and Williams, M. E. "Design and analysis framework for linear permanent-magnet machines," *IEEE Trans Ind Appl*, 1996, **32**, 371-379
- 3 Halbach, K. "Design of permanent multipole magnets with oriented rare earth cobalt material," *Nucl Instrum Meth*, 1980, **169**, 1-10
- 4 Kim, W.-J., Trumper, D. L. and Bryan, J. B. "Linear-motor-levitated stage for photolithography," *Ann CIRP*, 1997, **46**, 447-450
- 5 Holmes, M. L., Hocken, R. J. and Trumper, D. L. "A long-range scanning stage (the LORS project)," *Proceedings of 1997 ASPE annual meeting*, October 1997
- 6 Goldstein, H. *Classical Mechanics*. Reading, MA: Addison-Wesley, 1980, chap. 4
- 7 Ludwick, S. J. "Modeling and control of a six degree of freedom magnetic/fluidic motion control stage." Master's thesis, Massachusetts Institute of Technology, Cambridge, MA, February 1996